npg

ARTICLE

Transcytosis in the blood–cerebrospinal fluid barrier of the mouse brain with an engineered receptor/ligand system

Héctor R Méndez-Gómez[1,2], Albert Galera-Prat[3,4], Craig Meyers[1,2], Weijun Chen[1,2], Jasbir Singh[1,2], Mariano Carrión-Vázquez[3,4] and Nicholas Muzyczka[1,2]

Crossing the blood–brain and the blood–cerebrospinal fluid barriers (BCSFB) is one of the fundamental challenges in the development of new therapeutic molecules for brain disorders because these barriers prevent entry of most drugs from the blood into the brain. However, some large molecules, like the protein transferrin, cross these barriers using a specific receptor that transports them into the brain. Based on this mechanism, we engineered a receptor/ligand system to overcome the brain barriers by combining the human transferrin receptor with the cohesin domain from *Clostridium thermocellum*, and we tested the hybrid receptor in the choroid plexus of the mouse brain with a dockerin ligand. By expressing our receptor in choroidal ependymocytes, which are part of the BCSFB, we found that our systemically administrated ligand was able to bind to the receptor and accumulate in ependymocytes, where some of the ligand was transported from the blood side to the brain side.

Molecular Therapy — Methods & Clinical Development (2015) **2**, 15037; doi:10.1038/mtm.2015.37; published online 7 October 2015

INTRODUCTION

Being one of the most delicate organs of the body, the brain is well protected against potentially toxic substances by the blood–brain barrier (BBB) and the blood–cerebrospinal fluid barrier (BCSFB). As a result, the treatment of brain disorders is often limited by the inability of therapeutic drugs to cross either of these barriers from blood to brain. In fact, less than 2% of all potential neurotherapeutic drugs are able to cross them.[1] This problem remains a key obstacle despite decades of research and thus, there is much interest in devising methods to reach the brain more efficiently.

One of the most promising approaches to overcome this problem is to exploit the physiologic mechanisms that the brain barriers have to ensure that certain nutrients like iron or glucose reach the brain.[2] For large molecules like transferrin or insulin, there are specific receptors highly expressed on the cells of the BBB and BCSFB that transport them into the brain by a mechanism called receptor-mediated transcytosis; the ligand binds to the receptor on the blood side of the brain barrier, then it is internalized, transported to the brain side of the barrier, and released in the brain parenchyma or the cerebrospinal fluid (CSF).[3]

Based on this mechanism, we built an engineered-receptor/ligand system that would work as follows: the engineered-receptor would be expressed in the cells of the brain barriers, providing specificity for brain targeting. The ligand, which only recognizes our receptor, would be delivered systemically by intravenous injection. The ligand would bind to the receptor and the ligand/receptor complex would be transported from the blood to the brain side of the barriers. Hence, any molecule or nanoparticle attached to the ligand would gain access to the central nervous system compartment.

The receptor-ligand combination we chose comes from the anaerobic bacteria *Clostridium thermocellum*, which has a self-assembled multiprotein complex called cellulosome for degradation of plant cell walls.[4] Cellulosome assembly is mediated by a complementary pair of modules called cohesin and dockerin, which interact with high specificity and affinity. We hypothesized that by combining the bacterial cohesin–dockerin anchoring system with a mammalian receptor, it should be possible to create an engineered receptor/ligand system for the brain barriers with high affinity, high specificity, and transport capabilities.

In this study, we have evaluated in the mouse brain the binding and transcytosis properties of the cohesin–dockerin system combined with the human transferrin receptor (TfR). The engineered receptor was expressed in choroidal ependymocytes of the BCSFB, using a recombinant adeno-associated virus vector (rAAV). Subsequently, the ligand was injected systemically and brains were analyzed for receptor/ligand binding. We found robust binding of the ligand to the choroid plexus as well as entry of the ligand into ependymocytes and transport to their apical (brain side) membranes.

RESULTS

Ex vivo validation of the receptor/ligand system

Cohesin 7 from the CipA scaffoldin gene[5] was fused to the C-terminus of the human transferrin receptor (TfR). This construct

was then cloned into a rAAV serotype 9 (rAAV9) vector under the control of a hybrid CMV-β actin promoter (AAV9-TfR-cohesin) (Figure 1a). In theory, AAV transduction would allow the TfR-cohesin protein to be expressed in mammalian cells, the transferrin receptor would localize the TfR-cohesin protein to the cell surface, and cohesin would then act as the binding domain for a ligand with dockerin. Our ligand was a fusion protein of green fluorescent protein (GFP) with dockerin and to build it, the dockerin sequence from the Cel8A cellulAse gene[6] was fused to the C-terminus of the open
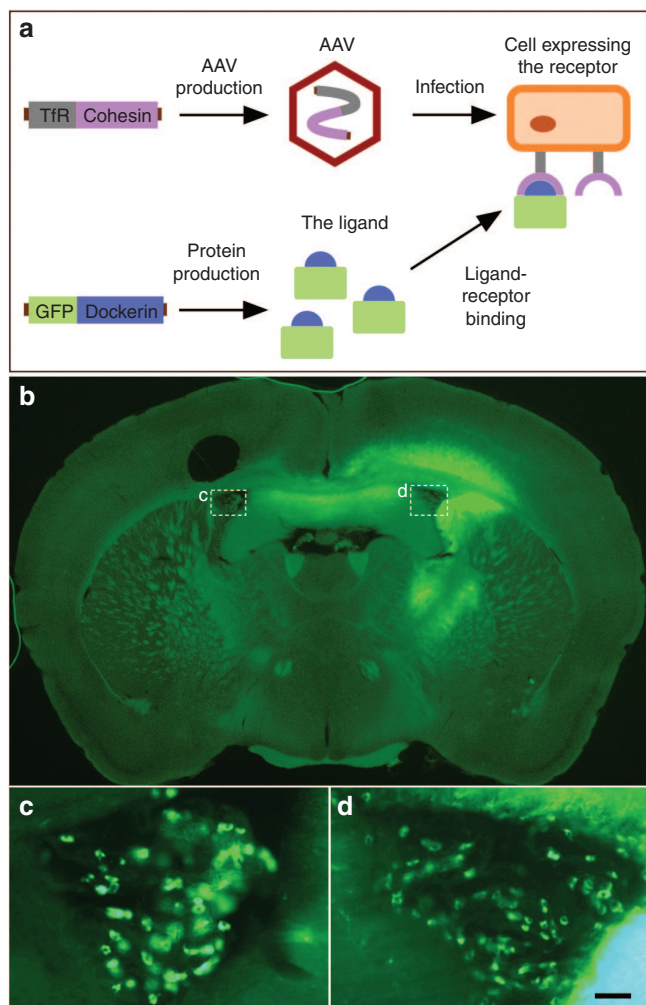
reading frame of the GFP (Figure 1a). The GFP-dockerin protein was then expressed in bacteria and purified as described in Methods. GFP was chosen to allow us to visualize the location of the GFP-dockerin protein after intravenous injection into animals expressing TfR-cohesin. The molecular weight of the GFP-dockerin molecule is approximately 37 kDa, which is not expected to cross the brain barriers. To test the receptor/ligand system, AAV9-TfR-cohesin was injected into the right ventricle or into the right striatum of mice. The left side in each case (ventricle or striatum) was left uninjected and used as a control.

To locate the expression of TfR-cohesin in the brain, and to determine if cohesin/dockerin binding functioned in brain tissue, brain slices from animals injected with TfR-cohesin were incubated in the presence or absence of GFP–dockerin 2 weeks post-rAAV injection. In animals injected in the right striatum, we found high GFP signal in the striatum and surrounding brain regions (Supplementary Figure S1b) following incubation with GFP-dockerin protein. As expected, slices incubated in the absence of GFP-dockerin showed no green signal (Supplementary Figure S1a).

In animals injected with AAV9-TfR-cohesin intraventricularly, we found a high green fluorescence signal in the brain parenchyma surrounding the right lateral ventricle, where the injection of AAV9-TfR-cohesin had occurred (Figure 1b). GFP signal was detected from the olfactory bulb/anterior olfactory nucleus to the hippocampus (Supplementary Figure S2), which reflects the degree to which the rAAV diffused from cerebrospinal fluid (CSF) into the surrounding brain parenchyma. In addition, we also found green signal in cells of the choroid plexus of the lateral ventricles, not only on the right side (Figure 1d) but also on the left side (Figure 1c). This was presumably due to the fact that choroid plexus cells in both ventricles were accessible to TfR-cohesin virus injected into the right ventricle via CSF.

To rule out the possibility that the AAV9 capsid or some portion of the TfR protein sequence were involved in GFP-dockerin binding, we made an alternative engineered receptor in which the human nerve growth factor receptor (NGFR) amino acid sequence was fused to cohesin and packaged in an AAV1 (rather than AAV9) serotype capsid (AAV1-NGFR-cohesin). When this rAAV virus was injected into the right striatum of the brain, we found strong GFP signal in the right striatum when brain slices were incubated with GFP-dockerin (Supplementary Figure S1d), and no signal in the absence of the GFP-dockerin ligand (Supplementary Figure S1c). This demonstrated that receptor/ligand binding was specific, i.e., due exclusively to the cohesin/dockerin interaction and not to a fortuitous binding of the GFP protein to the transferrin receptor or to components of the AAV capsid protein that might remain 2 weeks postinjection. These results also showed that both TfR-cohesin and NGFR-cohesin could be expressed on the membrane of mammalian cells, and that GFP-dockerin was able to bind TfR-cohesin and NGFR-cohesin in brain tissue, validating that the engineered receptor/ligand system was working correctly.

Ligand injected intravenously in vivo labels cells of the choroid plexus in the brain

The BBB and the BCSFB present several differences. The BBB is located in the brain parenchyma and it is formed by the endothelial cells of the capillaries in the brain parenchyma. These cells are connected by tight junctions that block the movement of molecules between blood and brain.[7] The endothelial cells are at the same time in contact with blood through their apical membrane and with the brain parenchyma through their basolateral membrane. The BCSFB, however, is located in the choroid plexus organs, which are located in the lateral ventricles as well as the third and fourth ventricles (Figure 2a). The

Figure 1 Expression of the engineered receptor following injection of the virus vector into a single brain ventricle. (**a**) Schematic representation of the receptor/ligand system. The receptor is a fusion protein of the human transferrin receptor (TfR) and the bacterial cohesin domain. The construct was cloned into a recombinant adeno-associated virus serotype 9 (rAAV9) vector to make AAV9-TfR-cohesin virus. The ligand is a fusion protein of green fluorescent protein (GFP) and the bacterial dockerin domain to make GFP-dockerin. GFP-dockerin is produced in bacterial culture and purified before use. (**b**) AAV9-TfR-cohesin vectors were injected in the right lateral ventricle of mouse brains. Two weeks later, brain slices were incubated with GFP-dockerin protein and GFP-dockerin binding with TfR-cohesin was analyzed by fluorescence microscopy to determine the cells that were expressing the receptor. Brain parenchyma near the right ventricle expressed higher levels of the receptor than the contralateral side, presumably because of the higher starting concentration of virus in CSF on the right side. (**c** and **d**) However, the virus concentration in CSF on both sides of the brain was sufficiently high to generate approximately the same level of receptor expression in choroid plexus cells on both sides of the brain. The hole marks the left side of the mouse brain. Scale bar (shown in **d**): (**b**) 0.72 mm; (**c,d**) 100 μm. CSF, cerebrospinal fluid.

choroid plexus is basically composed of a dense network of capillaries surrounded by a single layer of epithelial cells called choroidal ependymocytes, and they do not have the same structure as the BBB.[8] In the choroid plexus, the capillary endothelial cells lack tight junctions and instead the ependymocytes are the cells that are tightly connected, which blocks the movement of molecules from the blood to the brain. Hence, in this barrier, the choroid ependymocytes are the cells that are at the same time in contact with blood fluids and brain tissue. These cells however are oriented in the opposite way, with the basolateral membrane facing the blood side and the apical membrane facing the brain side. We hypothesized that if we could target and infect ependymocytes of the choroid plexus or endothelial cells in the brain parenchyma, we might be able to express the TfR-cohesin receptor on the side in contact with blood, so that GFP-dockerin

injected into the blood could potentially reach TfR-cohesin receptors and bind to them *in vivo*.

To test this hypothesis in the choroid plexus, AAV9-TfR-cohesin virus was injected into the right lateral ventricle of mouse brains. Two weeks later, a single tail vein injection of GFP-dockerin was performed and 8 hours later, brains were fixed and brain slices were analyzed by fluorescence microscopy. GFP signal was found in the choroid plexus of both lateral ventricles (Figure 2b and Figure 2c, arrows) as well as in the choroid plexus of the third (Figure 2c, arrowhead) and fourth ventricle (Figure 2d). However, no other GFP signal was found in other regions of the brain (not shown). Injection of GFP-dockerin without previous injection of AAV9-TfR-cohesin did not show any GFP signal, ruling out the possibility that GFP-dockerin was able to accumulate in the choroid plexus on its own (not shown).

To test our hypothesis on the endothelial cells of the brain parenchyma, which formed the BBB, we did the same experiment but injected AAV9-TfR-cohesin virus into the striatum. In this approach, the expectation was that rAAV would infect not only neural cells but also the endothelial cells of the capillary network of the brain parenchyma. This in turn would result in expression of TfR-cohesin on the apical (blood) side of brain endothelial cells near the injection site. Two weeks postvirus injection, a single tail vein injection of GFP-dockerin was performed and 8 hours later, brains were fixed and brain slices were analyzed by fluorescence microscopy. No GFP signal was found in brain parenchyma (not shown) suggesting that
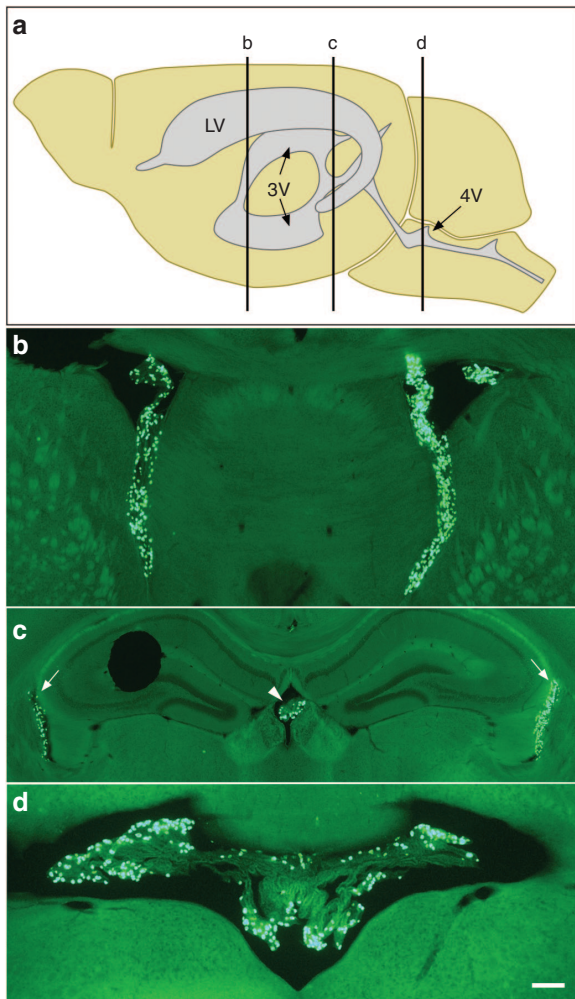

Figure 2 Green fluorescent protein (GFP)-dockerin binds cells from the choroid plexus in all ventricles of the brain *in vivo*. (**a**) Schematic representation of the ventricular system in the mouse brain showing the approximate positions of the lateral (LV), third (3V), and fourth (4V) ventricles. b, c, and d lines indicate the approximate location of the brain images shown in **b**, **c**, and **d** pictures. AAV9-TfR-cohesin vector was injected in the right lateral ventricle of mouse brains. Two weeks postvector injection, GFP-dockerin was injected intravenously into mice and GFP-dockerin binding with TfR-cohesin was analyzed by fluorescence microscopy in brain slices from regions **b**, **c**, and **d**. The images showed green signal from GFP-dockerin in the choroid plexus of lateral ventricles (**b**, **c** arrows), the third ventricle (**c** arrowhead), and the fourth ventricle (**d**). The hole marks the left side of the mouse brain. Scale bar (shown in **d**): (**b**) 265 μm, (**c**) 600 μm, (**d**) 295 μm.
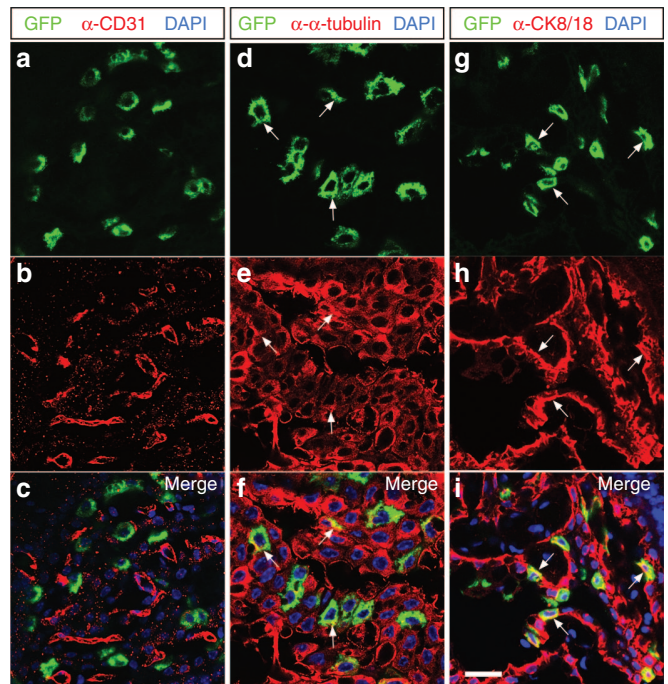

Figure 3 Type of cells binding green fluorescent protein (GFP)-dockerin in choroid plexus. Confocal images of mouse brain sections showing GFP-dockerin (green) bound to cells of the choroid plexus (**a**,**d**,**g**). The sections were also stained red with CD31 antibody (**b**), α-tubulin antibody (**e**), or cytokeratin 8/18 antibody (**h**). CD31 antibody labels endothelial cells of capillaries, while α-tubulin and cytokeratin 8/18 antibodies label the perinuclear cytoplasm of choroidal ependymocytes. **c** is merged from **a** and **b**, showing that no cells positive for CD31 were binding GFP-dockerin. However, **f** (merged from **d** and **e**), and **i** (merged from **g** and **h**) show partial colocalization of GFP-dockerin signal with α-tubulin and cytokeratin 8/18, respectively (arrows). Nuclei were also stained with 4′,6-diamidino-2-phenylindole (DAPI; blue) in **c**, **f**, and **i**. Scale bar (shown in **i**): (**a**–**c**) 33 μm, (**d**–**f**) 22 μm, (**g**–**i**) 30 μm.

GFP   Phalloidin   DAPI
α-GFP (only membrane)

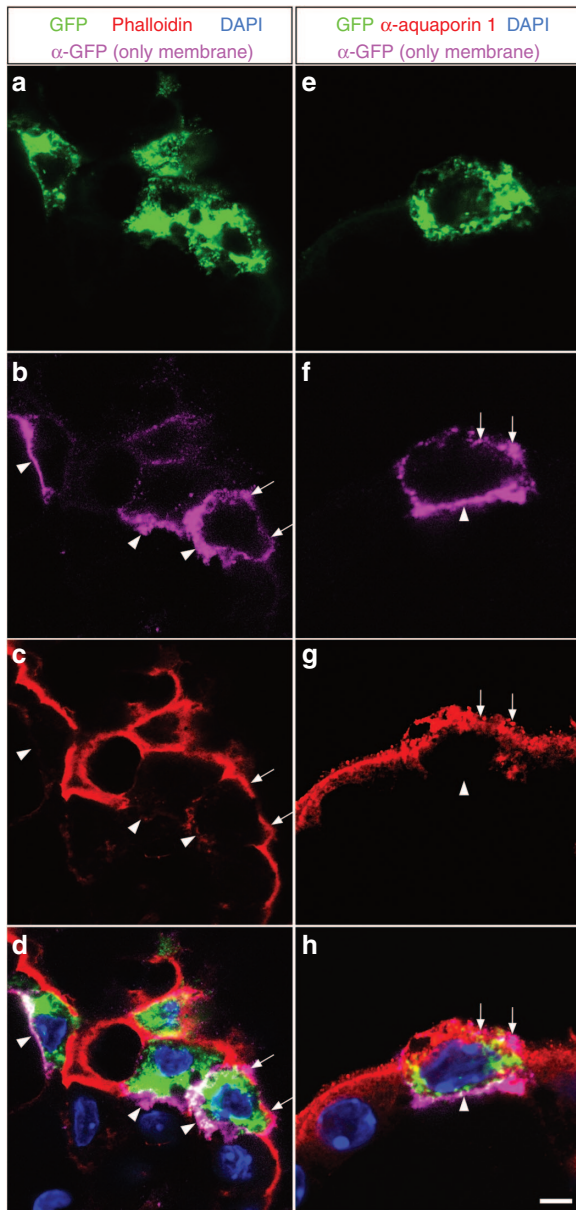GFP   α-aquaporin 1   DAPI
α-GFP (only membrane)

Figure 4   Membrane location of green fluorescent protein (GFP)-dockerin by confocal microscopy. (**a,e**) Confocal images of mouse brain sections showing green fluorescent signal of GFP-dockerin that was bound to or had entered the cytoplasm of choroidal ependymocytes. (**b,f**) GFP-dockerin located only on the cell membrane was visualized by staining with anti-GFP antibody (purple, α-GFP, only membrane). The apical membrane of choroidal ependymocytes was stained using fluorescent phalloidin (**c**, red) or aquaporin 1 antibody (**g**, red). **d** is merged from **a, b, c**; **h** is merged from **e, f, g. d** and **h** show GFP-dockerin receptor is present on the basolateral membrane (arrowheads) and also, at a lower level, on the apical membrane (arrows). Nuclei were stained with 4′,6-diamidino-2-phenylindole (DAPI; blue) in **d** and **h**. Scale bar (shown in **h**): (**a–d**) 6.6 μm, (**e–h**) 4.4 μm.

the endothelial cells of the BBB could not be infected by rAAV9 via the basolateral (brain) side. Alternatively, they could not express the TfR-cohesin cassette or the TfR-cohesin protein did not correctly traffic to the apical membrane. To be sure that the TfR-cohesin was actually expressed in the brain parenchyma of these animals, brain slices were incubated with GFP-dockerin. We found high GFP signal in the striatum and surrounding regions, as we showed previously (Supplementary Figure S1b).
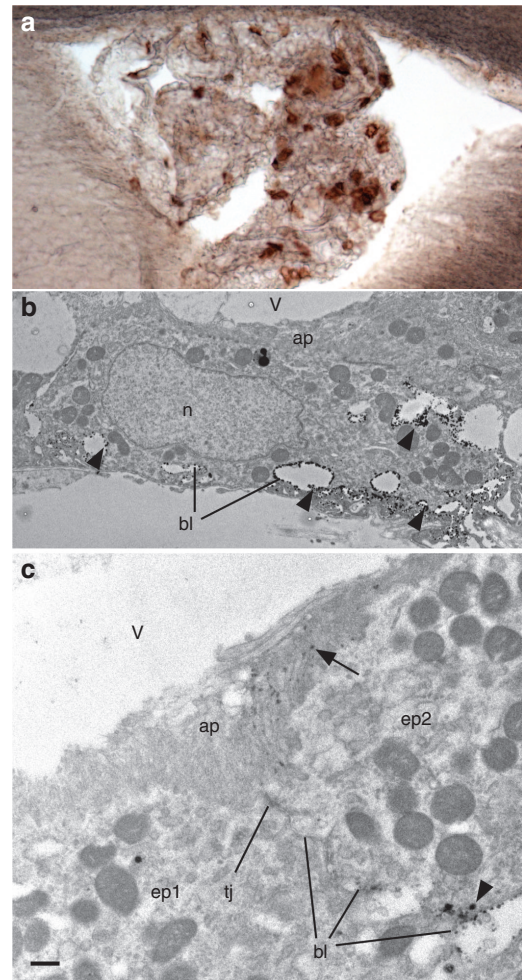

Figure 5   Membrane location of green fluorescent protein (GFP)-dockerin by electron microscopy. (**a**) Light microscopy image showing GFP-dockerin located only on the cell membrane using an anti-GFP antibody and peroxidase/DAB reaction. (**b**) Electron microscopy image showing the peroxidase/DAB reaction product in the cell membrane of a choroidal ependymocyte. Arrowheads show peroxidase/DAB reaction product on the basolateral membrane (bl). (**c**) Electron microscopy image of two ependymocytes, one unlabeled (ep1) and one labeled (ep2), showing both cellular sides, the flat and folded basolateral membrane (bl) and the apical membrane covered with cilia and microvilli (ap). The DAB reaction product, indicating GFP-dockerin, is present on both the basolateral membrane (arrowhead) as well as the apical membrane (arrow) of the choroidal ependymocyte. n, nucleus; ap, apical membrane (brain side); bl, basolateral membrane (blood side); V, cerebral ventricle; ep1, unlabeled ependymocyte; ep2, labeled ependymocyte; tj, tight junction. Scale bar (shown in **c**): (**a**) 50 μm, (**b**) 1.12 μm, (**c**) 0.5 μm. DAB, 3,3′-diaminobenzidine.

Together, these results show that when the receptor, TfR-cohesin, is expressed in cells of the choroid plexus organs, GFP-dockerin, injected intravenously, is able to bind and accumulate in those cells, confirming that the engineered receptor/ligand system works *in vivo*. Our attempt to express the receptor in capillary endothelial cells via brain parenchymal injection was, however, unsuccessful.

Ligand binds and enters choroidal ependymocytes
We next asked which cells of the choroid plexus were binding the GFP-dockerin ligand. As mentioned earlier, because choroid plexus is mainly composed of endothelial cells and choroidal ependymocytes, we performed immunostaining for these two kinds of cells. When we immunostained against CD31, a marker of endothelial
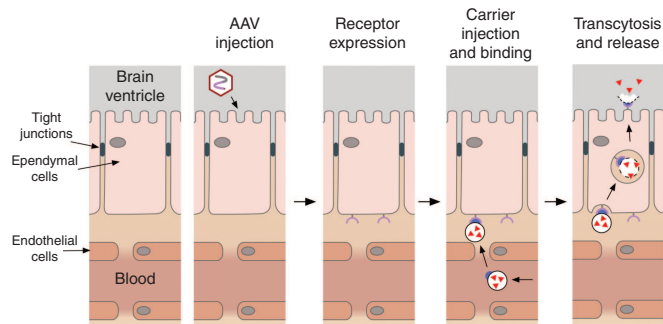
Figure 6 Brain delivery model of the engineered receptor/ligand system combined with a nanoparticle. Schematic representation of the blood–cerebrospinal fluid barrier (BCSFB) composed by ependymal cells (or ependymocytes) and tight junctions. The delivery system would work as follows: Injection of an adeno-associated virus vector carrying the engineered receptor would infect the ependymal cells of the choroid plexus. The ependymal cells of the BCSFB would express the receptor on the blood side of the barrier. Subsequently, the ligand attached to a nanoparticle would be injected intravenously. The carrier would bind to the receptor via the ligand, and the receptor would transport the nanoparticle to the brain side of the ependymal cells. During the transcytosis, the nanoparticle would release the cargo so when the vesicle fuses with the cellular membrane, the cargo would be released in the cerebrospinal fluid of the brain ventricles.

cells, we could not find colocalization of CD31 with GFP (Figure 3a–c). However, when we immunostained for two markers of choroidal ependymocytes, α-tubulin and cytokeratin 8/18 (ref. 9), colocalization with GFP-dockerin was seen for both ependymocyte markers (Figure 3d–i, arrows), indicating that the majority of the cells that were binding GFP-dockerin were choroidal ependymocytes. 3D confocal analysis showed that GFP-dockerin was not only on the membranes of choroidal ependymocytes but also throughout the cytosol of the cells (Supplementary Video S1), indicating that GFP-dockerin was being internalized into the ependymocytes, presumably via the transferrin receptor. These results demonstrated that systemically administered GFP-dockerin was binding specifically to choroidal ependymocytes and also that it was being internalized into the cytosol of these cells.

Ligand undergoes transcytosis in the blood–CSF barrier
We next addressed whether GFP-dockerin was present on the basolateral, apical, or both membranes of choroidal ependymocytes. The apical (or luminal) membrane faces the ventricles of the brain, while the basolateral membrane faces the capillary network, in close contact with blood. Choroidal ependymocytes are highly polarized cells and express different markers on each membrane side.[10] To perform the analysis, we used an anti-GFP antibody, which would highlight the GFP-dockerin located only on the membrane of the cells (Figure 4b,f). To identify the apical membrane, we used two markers: phalloidin coupled with a fluorochrome (Figure 4c) and an antibody against aquaporin 1 (Figure 4g). Phalloidin binds to F-actin, which is predominantly present in the apical border of ependymocytes,[9,11] and aquaporin 1 has also been found predominantly on the apical membrane.[12,13]

As shown earlier, the green fluorescence signal of GFP-dockerin was distributed throughout the cytosol of the ependymocytes (Figure 4a,e). GFP-dockerin labeling of the membrane showed that the ligand was distributed predominantly on one side of the membrane (compare arrowheads in Figure 4b,d, and in Figure 4f,h), presumably the basolateral membrane, because that part of the membrane showed lower levels of phalloidin

(Figure 4c,d, arrowheads) or aquaporin 1 signals (Figure 4g,h, arrowheads). However, we also found some membrane GFP signal that colocated with phalloidin (Figure 4b–d, arrows) and with Aquaporin 1 (Figure 4f–h, arrows), showing that some GFP-dockerin was located on the apical membrane of the ependymocytes, which is the brain side of the BCSFB. We quantified the proportion of cells with GFP-dockerin on the apical membrane and we found that 61.08% ± 23.42 (n = 4 animals) of the green cells had GFP-dockerin on the membrane colocating with Phalloidin (Figure 4d, arrows). Since GFP-dockerin had access only to the basolateral membrane, these observations suggested that GFP-dockerin entered from the basolateral side and was transported to the apical membrane of choroidal ependymocytes.

To confirm the results found by confocal microscopy, we examined the same samples by electron microscopy. GFP-dockerin was labeled by peroxidase/3,3'-diaminobenzidine (DAB) immunohistochemistry using an anti-GFP monoclonal antibody (Figure 5a). In the electron micrographs of the choroid plexus tissue, peroxidase activity was revealed by an electron-dense reaction product (Figure 5b, arrowheads). The brain and blood sides of choroid ependymocytes have different morphology: the apical (ap) (or luminal) membranes display cilia and dense microvilli (Figure 5b,c, ap), while the basal and lateral surfaces (bl) are flat with strongly folded labyrinths with the neighboring cells at the transition from lateral to basal surfaces (Figure 5b,c, bl). As expected, electron-dense particles corresponding to GFP-dockerin were detected in high number on the basolateral surfaces of ependymocytes (Figure 5b,c, arrowheads). However, we also found some cells with electron-dense particles on the apical membrane, between the microvilli (Figure 5c, arrow). This result confirmed the findings from the confocal microscopy experiments that some GFP-dockerin was located on the apical membrane of ependymocytes, suggesting that transcytosis of GFP-dockerin from the basolateral to the apical surface had occurred.

Taken together, these results demonstrate that GFP-dockerin injected into blood is able to bind to the TfR-cohesin expressed on the basolateral membrane of choroidal ependymocytes. Furthermore, the bound GFP-dockerin is internalized in the majority of the ependymocytes, and in some cells, GFP-dockerin is transported from the basolateral membrane (blood side) to the apical membrane (brain side), hence crossing the BCSFB.

DISCUSSION
Exploiting the receptor-mediated transcytosis mechanism of the brain barriers is a promising way to reach effectively the central nervous system. Unfortunately, the mechanism behind transcytosis is still poorly understood due in part to the lack of tools for its study and manipulation.

Conceptually, a unique receptor expressed only in the brain barriers and not in other tissues with a ligand that only targets that receptor would be an ideal method for studies of brain targeting and transcytosis.

With this idea in mind, we have built an engineered receptor-ligand system using the cohesin–dockerin domains from the bacterium *C. thermocellum* and a mammalian receptor. The cohesin and dockerin binding domains are small (cohesin = 143 aa, ~17 kDa; dockerin = 62 aa, ~7 kDa), simple, require no post-translational processing or lipid attachment, have dissociation constant that is comparable to high affinity antibodies (K_d between 10^{-8}–10^{-11} M)[14] and they are not present in animals.[15] The mammalian receptor chosen was the human transferrin receptor because it had been previously shown to mediate receptor-mediated transcytosis in the brain barriers.[16,17]

In this study, we have analyzed the binding and transcytosis capabilities of our receptor/ligand system in the mouse brain. The results show that cohesin and dockerin were binding *in vivo* in the choroid plexus (Figures 2 and 3), and that the TfR-cohesin/ GFP-dockerin complex was readily internalized in choroid ependy-mocytes (Figure 3 and Supplementary Video S1). Further, we found transcytosis of the GFP-dockerin ligand in the BCSFB (Figures 4 and 5). It is unlikely that binding of cohesin and dockerin triggers the internalization of the TfR-cohesin. Rather, it is possible that the cohesin/GFP-dockerin binding does not prevent the interaction of circulating endogenous transferrin with the TfR docking site of TfR-cohesin, which results in the entire complex including transferrin and GFP-dockerin being internalized. This phenomenon has been seen before when the transferrin receptor was targeted with antibodies that do not target the binding site for transferrin.[16,18]

Even though we found GFP-Dockerin located on the brain side of the barrier we could not determine if GFP-dockerin was released in the CSF. This result was anticipated due to the tight binding of the dockerin–cohesin domains and our findings support it by showing GFP-dockerin bound to the apical membrane of the ependymo-cytes. However, reversibility of cohesin–dockerin binding is not essential to achieve delivery into the central nervous system com-partment. A model of this delivery approach using a pH-sensitive nanoparticle as an example is illustrated in the Figure 6. In the case of the transferrin receptor, previous works have described that dur-ing its internalization the interior of the vesicle encounters a drop of the pH from 7.4 to 5.6 (ref. 19). Once the TfR-cohesin receptor brings a putative dockerin-nanoparticle into a cellular endosomal compartment where the pH lowers, the nanoparticle will release its contents into the vesicle. The vesicle in turn will be transcytosed and its contents will be released into the cerebrospinal fluid when it fuses with the apical membrane of the ependymal cells.

In this study, only the BCSFB could be targeted. When we tried to target the BBB, we found no evidence of GFP-dockerin binding in endothelial cells of this barrier. It has been shown that the AAV1 and AAV9 serotypes are able to infect endothelial cells when injected intravenously.[20,21] However, in our experiments, these AAV serotypes were not able to infect endothelial cells when AAV was injected into brain parenchyma. The high neural tropism of these AAV serotypes or the lack of receptors on the brain side of the endothelial cells for these serotypes could explain our results.

One of the drawbacks of targeting a physiologic receptor is that they are expressed not only in the brain barriers, but in other tissues of the body. A well-documented case is the transferrin receptor. This receptor is highly expressed in the brain barriers[22,23] but also in other organs,[24,25] so when, for instance, transferrin receptor is targeted with an antibody, the concentration of the antibody increases in the brain but the vast majority of the antibody ends up in other tissues, specifically the spleen and the liver.[26,27] As a result, this off-target effect reduces the efficiency of reaching the brain to the point where the fraction of molecules that ends up in the central nervous system is very low.[28] Since our receptor can be expressed exclusively in the brain barriers using the proper vector and promoter, both more effective brain targeting and less off-target effect should hap-pen. Whether dockerin nonspecifically binds to receptors in other tissues remains to be determined.

One of the limitations of our approach versus targeting physiologic receptors is that all the proteins of our system are foreign to the ani-mal host; so, an immune response is expected. Because of this, the use of the system presented in this study is limited to research purposes and any direct clinical application will require further development.

In summary, our experimental findings are, to the best of our knowledge, the first to demonstrate a proof of concept that an engi-neered receptor/ligand system could be a useful tool for studies of transcytosis *in vivo* and for brain delivery. Although effective brain targeting remains elusive, we expect that this new approach may help to solve the problem.

MATERIALS AND METHODS
Recombinant plasmids
pTR-TfR-cohesin. The cohesin open reading frame (143 amino acids (aa)) from pRSET-A_(I27)3-c7A-(I27)2 (ref. 29) was amplified using polymerase chain reaction (PCR) as a BamHI fragment (for a list of primers used in this study, see Supplementary Table S1) and inserted into pTfR-PAmCherry1 (ref. 30) (plasmid 31948; Addgene, Cambridge, MA), to produce the pTfR-cohesin-PAmCherry1 plasmid. To construct the pTR-TfR-cohesin plasmid, the TfR-cohesin open reading frame from pTfR-cohesin-PAmcherry1 was PCR amplified as a NotI-SalI fragment and cloned into pTR-UF11 (ref. 31), swapping it with the sequence containing the hGFP and neomycin-re-sistance genes. The final construct pTR-TfR-cohesin contains the coding sequences for human transferrin receptor fused in frame with the cohesin sequence at the C-terminal end of TfR under the control of the synthetic CBA promoter[32] and the human bovine growth hormone poly(A) site, all of it flanked by the AAV2 terminal repeats.

pTR-NGFR-cohesin. The cohesin-coding sequence was inserted in frame into the NGFR-coding sequence between the reticulum signal peptide of NGFR and receptor domain. The reticulum signal peptide (RSP) sequences of NGFR were purchased and the BamHI-XhoI fragment was inserted into a plasmid containing a multicloning site (MCS-plasmid). The NGFR open reading frame without the RSP (NoRSP-ΔNGFR) was PCR amplified from the plasmid ΔNGFR-2A-p47 (ref. 33), as a EcoRI-NotI fragment and inserted in the RSP-MCS-plasmid, in the same open reading frame as the RSP. The cohesin open reading frame was amplified as a XhoI-XhoI fragment and in-serted into the RSP-ΔNGFR-MCS-plasmid, between RSP and ΔNGFR in the same open reading frame, producing the RSP-cohesin-NGFR-MCS-plasmid. The fragment RSP-cohesin-NGFR was cut with NotI and SalI and inserted into the pRT-UF11 digested with NotI and SalI, swapping it with the se-quence containing the hGFP and neomycin-resistance genes to make pTR-NGFR-cohesin. The final pTR-NGFR-cohesin construct contains the coding sequences of human NGFR fused with cohesin under the control of the syn-thetic CBA promoter and the human bovine growth hormone poly(A) site, all of it flanked by the AAV2 terminal repeats.

pET28A-GFP-Dockerin. The *C. thermocellum* dockerin sequence (containing also the linker separating the catalytic unit from the dockerin, at the 5' end) was PCR amplified from pET28-Cel8A.[34] The EcoRI/XhoI fragment containing the linker separating the catalytic unit from the dockerin (at the 5') and stop codon insertion before the Xhol site was cloned into a pET28a vector (No-vagen, Madison, WI). The coding sequence for GFP was PCR amplified from (Hys)6-GFP-ssrA,[35] as an NdeI/EcoRI fragment and cloned into pET28-dockerin. The resulting construct codes for a protein containing a poly-histidine tag (His-tag), GFP, the linker and dockerin, all in the same reading frame.

GFP-dockerin protein production
Escherichia coli enhanced BL21 strain (T7 express lysY, New England Biolabs, Ipswich, MA) containing pET28A-GFP-dockerin was grown in 500 ml LB with 50 μg/ml kanamycin and grown for 4 hours at 30 °C. Subsequently, isopropyl-β-D-thiogalactopyranose was added at a final concentration of 0.5 mmol/l and culture growth was continued for 20 hours at 16 °C to induce protein expression. Cells were harvested by cen-trifugation (6,000 g for 15 minutes at 4 °C) and resuspended in 20 ml of His buffer (50 mmol/l Tris pH 7.65, 25 mmol/l NaCl, 2 mmol/l CaCl$_2$) sup-plemented with protease inhibitors (phenylmethylsulfonyl fluoride 0.5 mmol/l, pepstatin A 5 μg/ml, chymostatin 1 μg/ml, leupeptin 1 μg/ml, aprotinin 2 μg/μl) and lysed with a French Press at 1,200 psi of pressure. The lysate was centrifuged (20,000 g for 30 minutes at 4 °C), and the supernatant was loaded onto a 5 ml HisTrap HP column (GE Healthcare Life Sciences, Pittsburgh, PA), pre-equilibrated with His buffer. Proteins were eluted in His buffer using a 30 ml linear gradient of 0–200 mmol/l imidazole. Fractions were collected, analyzed (see below), and loaded onto a 5 ml Hitrap Q HP column (GE Healthcare Life Sciences), pre-equilibrated with Q buffer (25

mmol/l Tris-HCl pH 8.5, 1 mmol/l DTT, 1 mmol/l CaCl$_2$) with protease inhibitor cocktail. GFP-dockerin was eluted in Q buffer using a linear gradient of 0–500 mmol/l NaCl. Analysis of the fractions were performed using a fluorometer to measure GFP signal (excitation filter: 485 ± 20 nm, emission filter: 528 ± 20 nm) and by SDS/PAGE with Comassie staining. The fractions containing relatively pure protein were pooled and dialyzed against phosphate-buffered saline (PBS) pH 8.0 and concentrated in an Apollo 20 kDa concentrator (Orbital Biosciences, Topsfield, MA) in 0.1M PBS pH 8.0. The GFP-dockerin was aliquoted and stored at −20 °C.

Production of rAAV

rAAV was isolated essentially as described,[36] with minor modifications. For the production of AAV9-TfR-cohesin, the plasmid pIM45-9 that expresses AAV2 rep and the AAV9 cap, was cotransfected using PEI[37,38] into HEK-293 cells with pTR-TfR-cohesin and pXX6 (ref. 39), which contains the adenovirus E4, VA, and E2a helper regions, to produce the AAV9-TfR-cohesin virus. The recombinant virus was purified by iodixanol step gradient, followed by vector concentration and buffer exchange with lactated Ringer's in an Apollo 150 kDa concentrator (Orbital Biosciences). The virus was stored at −80 °C. AAV1-NGFR-cohesin, was produced by the same method, but using the plasmids pXYZ1 (ref. 36) and pTR-NGFR-cohesin during the transfection. Virus titers (vector genomes per ml) were determined by dot blot: AAV1-NGFR-cohesin = 2.47 × 10^{12} vg/ml. AAV9-TfR-cohesin = 5.58 × 10^{12} vg/ml.

Animals

The animal procedures were performed according to a protocol approved by the Institutional Animal Care and Use Committee at the University of Florida. Balb/cj strain mice 4–5 weeks of age were used for the experiments.

Intracerebral injection of AAVs

All surgical procedures were performed using aseptic techniques and isoflurane gas anesthesia. After mice were anesthetized, they were placed in the stereotactic frame (Kopf Instruments, Tujunga, CA), and rAAV vectors were injected into either the right Striatum (Str) (anterior–posterior (AP) −0.3 mm, lateral (lat) −2.0 mm, dorsoventral (DV) −3.0 mm) or the right lateral ventricle (LV) (AP −0.3 mm, Lat −1.0 mm, DV −2.0 mm), through a glass micropipette with an inner diameter ~30–40 µm at a rate of 0.5 µl/minute. Animals were injected with a total of 2 µl of virus in the Str or 10 µl in the LV. The needle was left in place for 5 minutes prior to withdrawal from the brain.

Systemic injection of GFP-dockerin

After the animals were anesthetized with isoflurane, a single dose of 100 µl of GFP-dockerin (3 µg/µl) was administrated via the tail vein, using an insulin syringe (30G × 1/2") (Easy Touch, Fairfield, OH) over a period of 30 seconds. Animals were perfused 8 hours later.

Brain tissue preparation

Animals were deeply anesthetized with pentobarbital (Beuthanasia-D, Merck, Kenilworth, NJ) and perfused through the ascending aorta. Brains were perfused with 10 ml of saline solution, followed by 10 ml of ice-cold 4% paraformaldehyde in 0.1 M phosphate buffer, pH 7.4. Brains were removed and postfixed overnight at 4 °C in paraformaldehyde solution.

Forty-micrometer-thick brain coronal sections (40 µm) were cut on a vibratome (Leica Microsystems, Wetzlar, Germany) and mounted for fluorescence microscopy analysis or processed for GFP-dockerin incubation or immunohistochemistry.

GFP-dockerin incubation

Brain sections were incubated overnight at 4 °C with 0.02 mg/ml of dockerin-GFP, 0.1% Triton-X100 (T9284, Sigma-Aldrich, St Louis, MO) and 3% goat serum (01-6201, Life Technologies, Carlsbad, CA). Brain sections were mounted on slides with Mowiol 4–88 (81381, Sigma-Aldrich). Samples were examined with a fluorescence stereomicroscope or a fluorescence microscope (Leica Microsystems) and images were processed with Pixelmator software (UAB Pixelmator Team, Vilnius, Lituania).

Immunohistochemistry for confocal microscopy

Immunostaining were carried out on free-floating sections as follows: Incubation with 0.1% Triton-X100 (T9284, Sigma-Aldrich), 3% goat serum (01-6201, Life Technologies) or donkey serum (D9663, Sigma-Aldrich) in PBS

for 1 hour at room temperature (RT); incubation with Phalloidin–Atto 565 (94072, Sigma-Aldrich) or one of the primary antibodies 4 °C overnight: rabbit anti-α Tubulin (ab18251, Abcam, Cambridge, MA) diluted 1:500, guinea pig anti-cytokeratin 8/18 (GP11, Progen Biotechnik, Heidelberg, Germany) diluted 1:100, rabbit anti-CD31 (ab28364, Abcam) diluted 1:100 or rabbit anti-Aquaporin 1 (ab15080, Abcam) diluted 1:125; 3 washes with PBS for 10 minutes each wash; incubation with one of the secondary antibodies for 2 hours at RT: Alexa Fluor555 donkey anti-Rabbit (A-31572, Life Technologies) diluted 1:500 or Alexa Fluor555 goat anti-Guinea Pig (A-21435, Life Technologies) diluted 1:500. Sections were then incubated with 4′,6-diamidino-2-phenylindole at 1 µg/ml for 10 minutes, washed with PBS three times for 10 minutes each wash, mounted on slides with Mowiol 4–88 and examined with a confocal microscope Leica TCS SP5 (Leica Microsystems).

To label GFP that was present only on the surface of the membranes, sections were stained without Triton-X100, as follows: Incubation with 3% goat serum (01-6201, Life Technologies) in PBS for 1 hour at RT; incubation with the primary rat anti-GFP (04404-84, Nacalai USA, San Diego, CA) diluted 1:1,000 at 4 °C overnight; three washes with PBS for 10 minutes each wash; incubation with the secondary Alexa Fluor647 goat anti-Rat (A-21247, Life Technologies) for 2 hours at RT; three washes with PBS for 10 minutes each wash; incubation of the slices with 4% paraformaldehyde; three washes with PBS for 10 minutes each wash. Once the GFP membrane staining was complete, the sections were stained for the other marker using Triton X-100, following the procedure described above, for Aquaporin 1 or Phalloidin.

To label GFP on the surface of membranes for electron microscopy, sections were processed as follows: incubation with 0.5% H$_2$O$_2$, 10% Methanol in PBS for 15 minutes; three washes of 10 minutes each with PBS; incubation with 1% goat serum in PBS for 1 hour at RT; incubation with primary rat anti-GFP antibody diluted 1:500 at 4 °C overnight; three washes with PBS for 10 minutes each wash; incubation with the secondary biotinylated goat anti-rat *antibody* (BA-9401, Vector Laboratories, Burlingame, CA) diluted 1:500 for 2 hours at RT; three washes of 10 minutes each with PBS; incubation with VECTASTAIN Elite ABC Kit (PK-6100, Vector Laboratories, Burlingame, CA) for 1 hour at RT; three washes with PBS for 10 minutes each wash. The sections were then stained using the NovaRED Peroxidase (HRP) Substrate Kit (SK-4800, Vector Laboratories) for 10 minutes, washed and processed for electron microscopy as described below.

Colocalization analysis

The proportion GFP+ cells with colocalization between membrane-GFP and Phalloidin labeling was performed as previously described.[40] Briefly, confocal z-stacks were taken from four microscopy fields per section, one section per animal, four animals. Each z-stack was individually analyzed and colocalization between membrane-GFP and Phalloidin were counted manually using ImageJ software (NIH, Bethesda, MD). Subsequently, the average of the four fields was used to represent each animal.

Electron microscopy

Transmission electron microscopy was carried out at the Interdisciplinary Center for Biotechnology Research Electron Microscopy Core as described previously.[41] After immunohistochemistry, sections were postfixed with 1% osmium tetroxide, dehydrated and embedded in EMbed812/Araldite epoxy resin. Ultrathin sections (100 nm) were then cut from the block surface, collected on 100 mesh carbon coated Formvar copper grids, and examined in an FEI Spirit LaB$_6$ 120kV transmission electron microscope (FEI, Hillsboro, OR) equipped with a Gatan Ultrascan 1000XP, 2k × 2k CCD digital camera (Gatan, Pleasanton, CA).

REFERENCES

1. Pardridge, WM (2005). The blood-brain barrier: bottleneck in brain drug development. *NeuroRx* **2**: 3–14.

2. Georgieva, JV, Hoekstra, D and Zuhorn, IS (2014). Smuggling drugs into the brain: an overview of ligands targeting transcytosis for drug delivery across the blood-brain barrier. *Pharmaceutics* **6**: 557–583.

3. Xiao, G and Gan, LS (2013). Receptor-mediated endocytosis and brain delivery of therapeutic biologics. *Int J Cell Biol* **2013**: 703545.

4. Bayer, EA, Belaich, JP, Shoham, Y and Lamed, R (2004). The cellulosomes: multienzyme machines for degradation of plant cell wall polysaccharides. *Annu Rev Microbiol* **58**: 521–554.

5. Gerngross, UT, Romaniec, MP, Kobayashi, T, Huskisson, NS and Demain, AL (1993). Sequencing of a Clostridium thermocellum gene (cipA) encoding the cellulosomal SL-protein reveals an unusual degree of internal homology. *Mol Microbiol* **8**: 325–334.

6. Anbar, M, Gul, O, Lamed, R, Sezerman, UO and Bayer, EA (2012). Improved thermostability of Clostridium thermocellum endoglucanase Cel8A by using consensus-guided mutagenesis. *Appl Environ Microbiol* **78**: 3458–3464.

7. Abbott, NJ, Rönnbäck, L and Hansson, E (2006). Astrocyte-endothelial interactions at the blood-brain barrier. *Nat Rev Neurosci* **7**: 41–53.

8. Damkier, HH, Brown, PD and Praetorius, J (2013). Cerebrospinal fluid secretion by the choroid plexus. *Physiol Rev* **93**: 1847–1892.

9. Li, YC, Bai, WZ, Sakai, K and Hashikawa, T (2009). Fluorescence and electron microscopic localization of F-actin in the ependymocytes. *J Histochem Cytochem* **57**: 741–751.

10. Christensen, IB, Gyldenholm, T, Damkier, HH and Praetorius, J (2013). Polarization of membrane associated proteins in the choroid plexus epithelium from normal and slc4a10 knockout mice. *Front Physiol* **4**: 344.

11. Li, YC, Bai, WZ and Hashikawa, T (2007). Regionally varying F-actin network in the apical cytoplasm of ependymocytes. *Neurosci Res* **57**: 522–530.

12. Speake, T, Freeman, LJ and Brown, PD (2003). Expression of aquaporin 1 and aquaporin 4 water channels in rat choroid plexus. *Biochim Biophys Acta* **1609**: 80–86.

13. Longatti, PL, Basaldella, L, Orvieto, E, Fiorindi, A and Carteri, A (2004). Choroid plexus and aquaporin-1: a novel explanation of cerebrospinal fluid production. *Pediatr Neurosurg* **40**: 277–283.

14. Slutzki, M, Barak, Y, Reshef, D, Schueler-Furman, O, Lamed, R and Bayer, EA (2012). Indirect ELISA-based approach for comparative measurement of high-affinity cohesin-dockerin interactions. *J Mol Recognit* **25**: 616–622.

15. Peer, A, Smith, SP, Bayer, EA, Lamed, R and Borovok, I (2009). Noncellulosomal cohesin- and dockerin-like modules in the three domains of life. *FEMS Microbiol Lett* **291**: 1–16.

16. Pardridge, WM, Buciak, JL and Friden, PM (1991). Selective transport of an anti-transferrin receptor antibody through the blood-brain barrier in vivo. *J Pharmacol Exp Ther* **259**: 66–70.

17. Friden, PM, Walus, LR, Musso, GF, Taylor, MA, Malfroy, B and Starzyk, RM (1991). Anti-transferrin receptor antibody and antibody-drug conjugates cross the blood-brain barrier. *Proc Natl Acad Sci USA* **88**: 4771–4775.

18. Jefferies, WA, Brandon, MR, Williams, AF and Hunt, SV (1985). Analysis of lymphopoietic stem cells with a monoclonal antibody to the rat transferrin receptor. *Immunology* **54**: 333–341.

19. Dhungana, S, Taboy, CH, Zak, O, Larvie, M, Crumbliss, AL and Aisen, P (2004). Redox properties of human transferrin bound to its receptor. *Biochemistry* **43**: 205–209.

20. Chen, S, Kapturczak, M, Loiler, SA, Zolotukhin, S, Glushakova, OY, Madsen, KM *et al.* (2005). Efficient transduction of vascular endothelial cells with recombinant adeno-associated virus serotype 1 and 5 vectors. *Hum Gene Ther* **16**: 235–247.

21. Varadi, K, Michelfelder, S, Korff, T, Hecker, M, Trepel, M, Katus, HA *et al.* (2012). Novel random peptide libraries displayed on AAV serotype 9 for selection of endothelial cell-directed gene transfer vectors. *Gene Ther* **19**: 800–809.

22. Roberts, RL, Fine, RE and Sandra, A (1993). Receptor-mediated endocytosis of transferrin at the blood-brain barrier. *J Cell Sci* **104 (Pt 2)**: 521–532.

23. Moos, T and Morgan, EH (2000). Transferrin and transferrin receptor function in brain barrier systems. *Cell Mol Neurobiol* **20**: 77–95.

24. Newman, R, Schneider, C, Sutherland, R, Vodinelich, L and Greaves, M (1982). The transferrin receptor. *Trends in Biochemical Sci* **7**: 397–400.

25. Lu, JP, Hayashi, K and Awai, M (1989). Transferrin receptor expression in normal, iron-deficient and iron-overloaded rats. *Acta Pathol Jpn* **39**: 759–764.

26. Moos, T and Morgan, EH (2001). Restricted transport of anti-transferrin receptor antibody (OX26) through the blood-brain barrier in the rat. *J Neurochem* **79**: 119–129.

27. Shi, N, Boado, RJ and Pardridge, WM (2001). Receptor-mediated gene targeting to tissues *in vivo* following intravenous administration of pegylated immunoliposomes. *Pharm Res* **18**: 1091–1095.

28. Ko, YT, Bhattacharya, R and Bickel, U (2009). Liposome encapsulated polyethylenimine/ODN polyplexes for brain targeting. *J Control Release* **133**: 230–237.

29. Valbuena, A, Oroz, J, Hervás, R, Vera, AM, Rodríguez, D, Menéndez, M *et al.* (2009). On the remarkable mechanostability of scaffoldins and the mechanical clamp motif. *Proc Natl Acad Sci USA* **106**: 13791–13796.

30. Subach, FV, Patterson, GH, Manley, S, Gillette, JM, Lippincott-Schwartz, J and Verkhusha, VV (2009). Photoactivatable mCherry for high-resolution two-color fluorescence microscopy. *Nat Methods* **6**: 153–159.

31. Zolotukhin, S, Potter, M, Hauswirth, WW, Guy, J and Muzyczka, N (1996). A "humanized" green fluorescent protein cDNA adapted for high-level expression in mammalian cells. *J Virol* **70**: 4646–4654.

32. Xu, L, Daly, T, Gao, C, Flotte, TR, Song, S, Byrne, BJ *et al.* (2001). CMV-beta-actin promoter directs higher expression from an adeno-associated viral vector in the liver than the cytomegalovirus or elongation factor 1 alpha promoter and results in therapeutic levels of human factor X in mice. *Hum Gene Ther* **12**: 563–573.

33. Wohlgensinger, V, Seger, R, Ryan, MD, Reichenbach, J and Siler, U (2010). Signed outside: a surface marker system for transgenic cytoplasmic proteins. *Gene Ther* **17**: 1193–1199.

34. Anbar, M, Lamed, R and Bayer, E (2010). Thermostability enhancement of *Clostridium thermocellum* cellulosomal endoglucanase Cel8A by a single glycine substitution. *ChemCatChem* **2**: 997–1003.

35. Benaroudj, N and Goldberg, AL (2000). PAN, the proteasome-activating nucleotidase from archaebacteria, is a protein-unfolding molecular chaperone. *Nat Cell Biol* **2**: 833–839.

36. Zolotukhin, S, Potter, M, Zolotukhin, I, Sakai, Y, Loiler, S, Fraites, TJ Jr *et al.* (2002). Production and purification of serotype 1, 2, and 5 recombinant adeno-associated viral vectors. *Methods* **28**: 158–167.

37. Choi, VW, Asokan, A, Haberman, RA and Samulski, RJ (2007). Production of recombinant adeno-associated viral vectors f\or *in vitro* and *in vivo* use. *Curr Protoc Mol Biol* **Chapter 16**: Unit 16.25.

38. Lock, M, Alvira, M, Vandenberghe, LH, Samanta, A, Toelen, J, Debyser, Z *et al.* (2010). Rapid, simple, and versatile manufacturing of recombinant adeno-associated viral vectors at scale. *Hum Gene Ther* **21**: 1259–1271.

39. Xiao, X, Li, J and Samulski, RJ (1998). Production of high-titer recombinant adeno-associated virus vectors in the absence of helper adenovirus. *J Virol* **72**: 2224–2232.

40. Méndez-Gómez, HR, Vergaño-Vera, E, Abad, JL, Bulfone, A, Moratalla, R, de Pablo, F *et al.* (2011). The T-box brain 1 (Tbr1) transcription factor inhibits astrocyte formation in the olfactory bulb and regulates neural stem cell fate. *Mol Cell Neurosci* **46**: 108–121.

41. Tremblay, ME, Riad, M and Majewska, A (2010). Preparation of mouse brain tissue for immunoelectron microscopy. *J Vis Exp* **41**: 2021.

Supplementary Information accompanies this paper on the *Molecular Therapy—Methods & Clinical Development* website (http://www.nature.com/mtm)